Cell Reports, Volume *8*

Supplemental Information

Autophagy Impairment in Muscle Induces Neuromuscular Junction Degeneration and Precocious Aging

Silvia Carnio, Francesca LoVerso, Martin Andres Baraibar, Emanuela Longa, Muzamil Majid Khan, Manuela Maffei, Markus Reischl, Monica Canepari, Stefan Loefler, Helmut Kern, Bert Blaauw, Bertrand Friguet, Roberto Bottinelli, Rüdiger Rudolf, and Marco Sandri

SUPPLEMENTAL DATA

Supplemental Figures

Figure S1

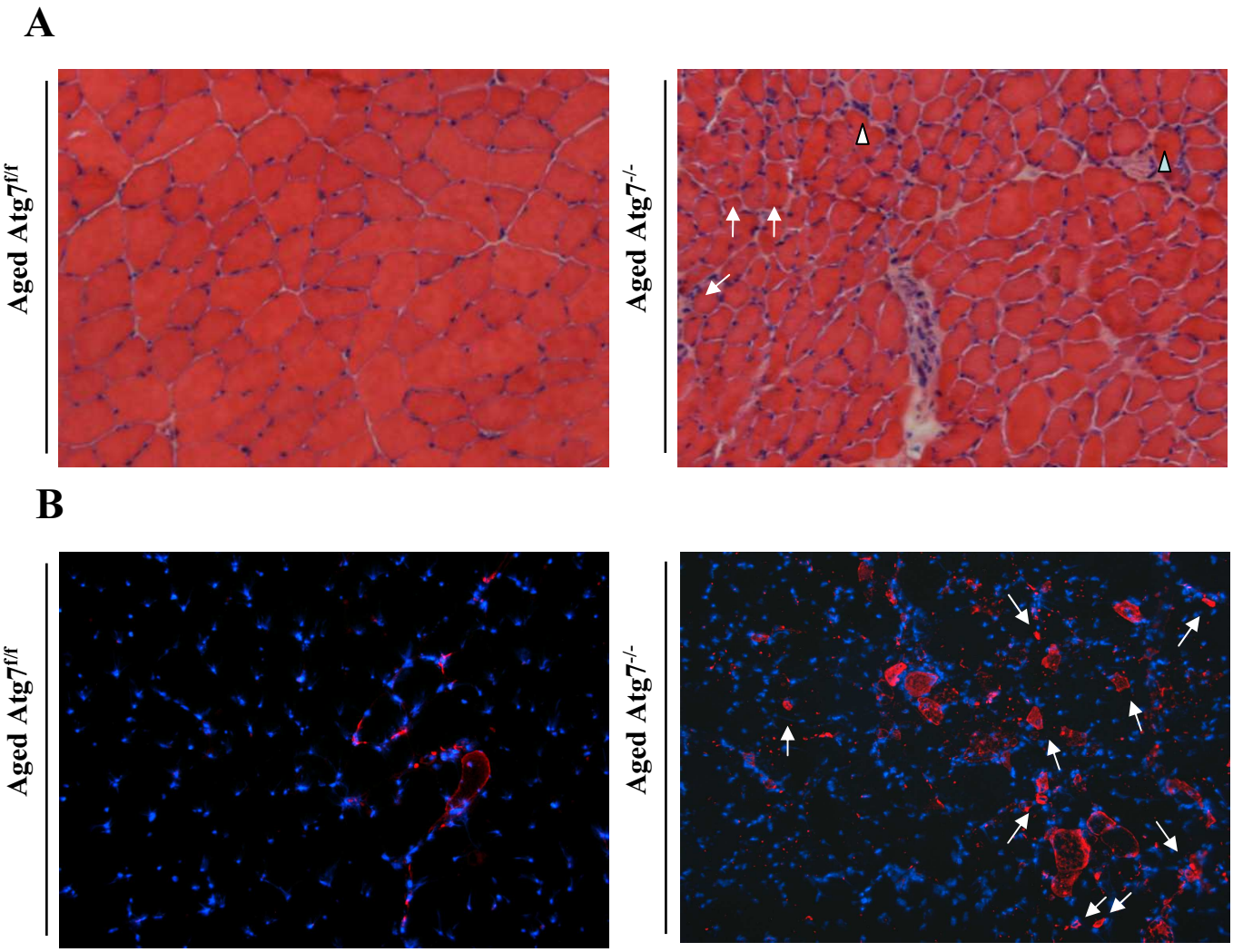

Figure S2

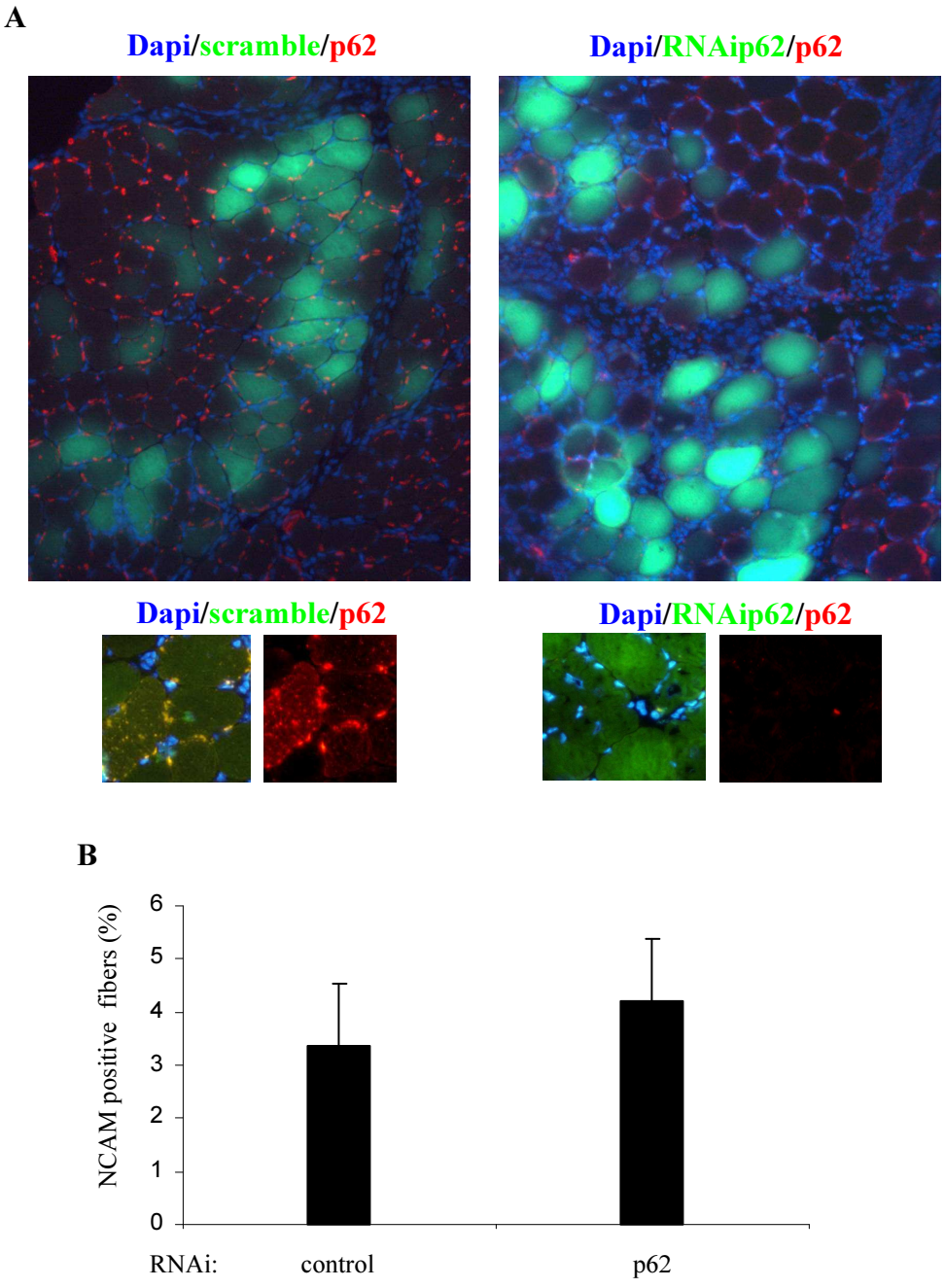
A
Dapi/scramble/p62
Dapi/RNAip62/p62
Dapi/scramble/p62
Dapi/RNAip62/p62
B
NCAM positive fibers (%)
0
1
2
3
4
5
6
RNAi:
control
p62

Figure S3

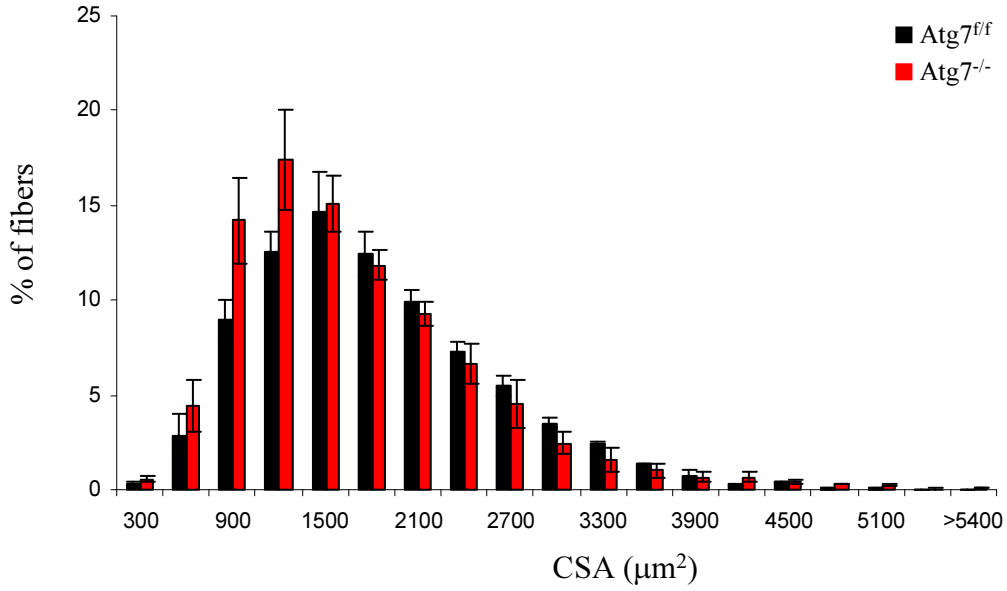
25
20
15
10
5
0
% of fibers
Atg7f/f
Atg7-/-
300
900
1500
2100
2700
3300
3900
4500
5100
>5400
CSA (µm2)

Figure S4

A

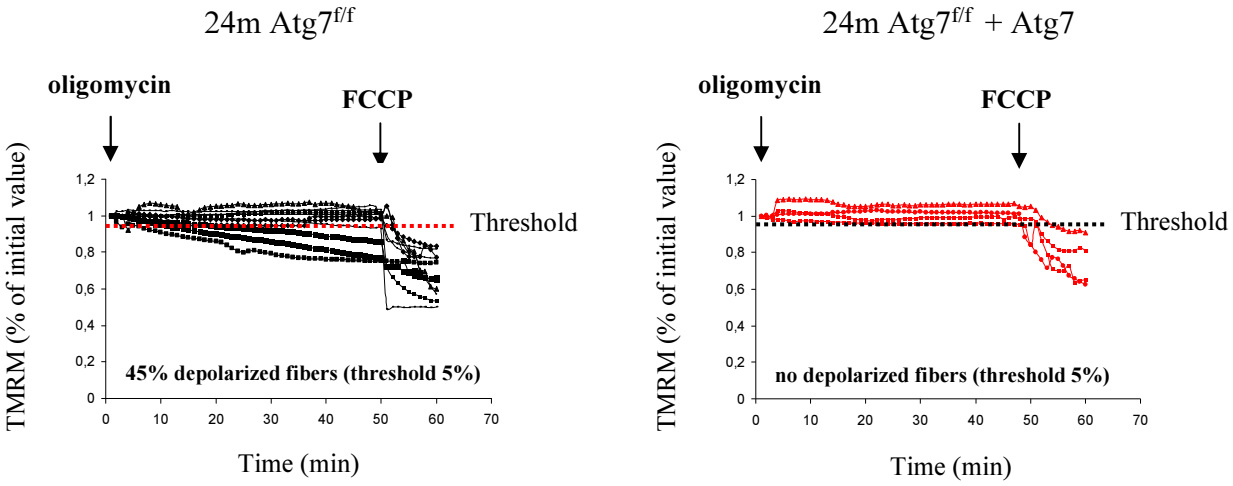

B

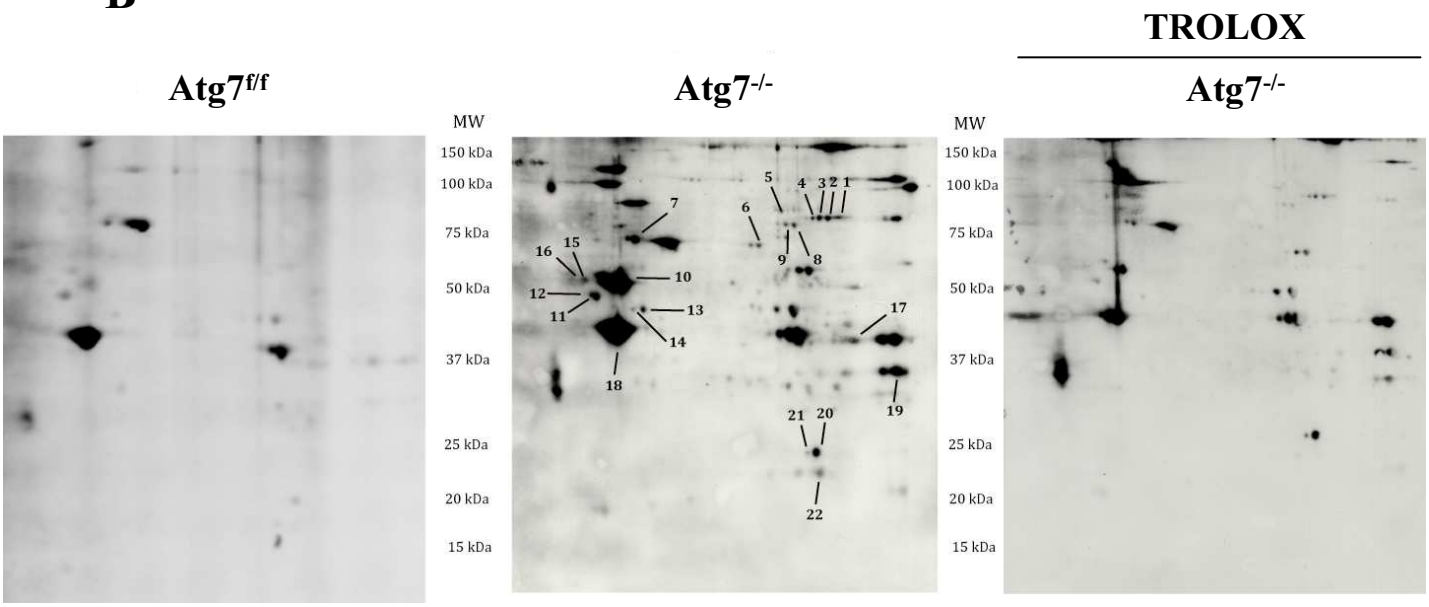

C

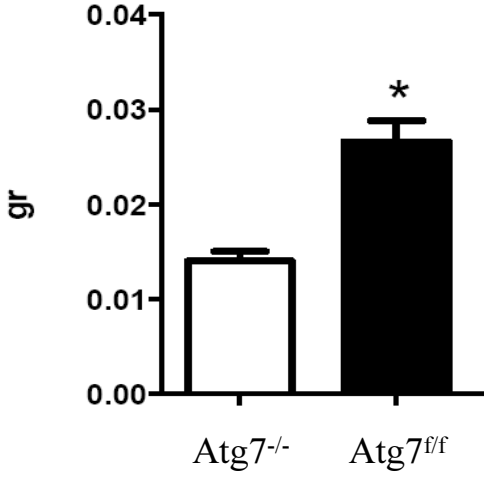

Atg7$^{-/-}$

Mean	SD	N
0.014040	0.004623	21

Atg7$^{f/f}$

Mean	SD	N
0.026606	0.008957	16

Figure S5

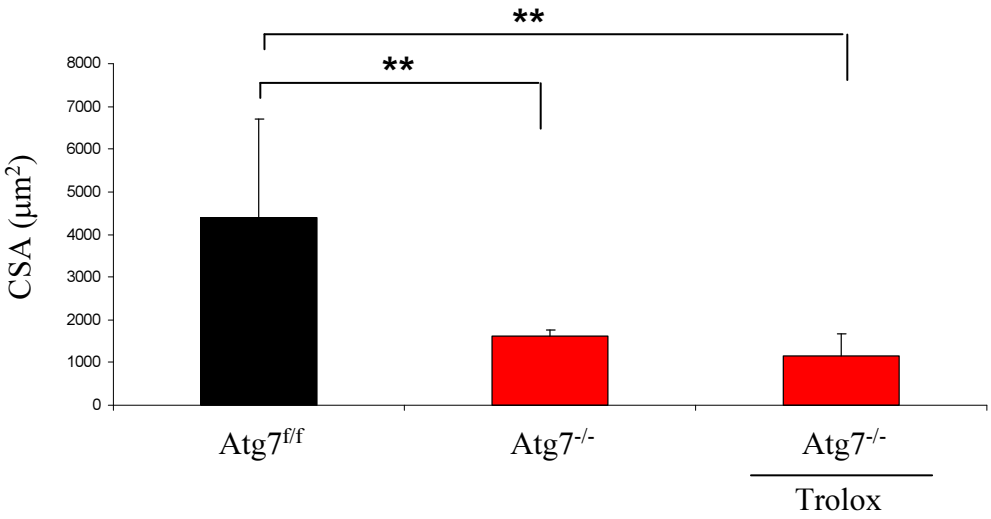
**
**
8000
7000
6000
5000
4000
3000
2000
1000
0
CSA (μm2)
Atg7f/f
Atg7-/-
Atg7-/-
Trolox

Figure S1. Morphological and functional impairment in muscles of *Atg7*$^{-/-}$ mice, related to Figure 2.

A. H&E staining of aged *Atg7*$^{f/f}$ and *Atg7*$^{-/-}$ Tibialis Anterior (TA) muscles shows that *Atg7*$^{-/-}$ muscles are atrophic with interstitial inflammation and center-nucleated fibers.

B. Representative images of immunostaining for Neural Cell Adhesion Molecule (NCAM) expression in aged *Atg7*$^{f/f}$ and *Atg7*$^{-/-}$ mice. Localization of NCAM along the entire fibers underlines the loss of muscle-nerve interaction.

Figure S2. Changes in NMJ are not secondary to p62 accumulation into aggregates, related to Figure 3.

A. Representative images of immunostaining for p62, that was knocked down *in vivo* in *Atg7*$^{-/-}$ mice, to reduce its content and the aggregates.

B. Quantification of NCAM positive fibers. Despite the absence of p62-positive aggregates, the percentage of denervated NCAM-positive fibers was not ameliorated.

Figure S3. Distribution of Cross Sectional Area in aged inducible *Atg7*$^{-/-}$, related to Figure 4.

Fiber size distribution analysis after acute *Atg7* deletion in aged mice revealed an enrichment in small fibers when compared to controls.

Figure S4. Autophagy is critical for mitochondrial function, oxidative stress and force generation, related to Figure 6.

A. TMRM analysis of mitochondria from aged *Atg7*$^{-/-}$ mice transfected with (right) or without (left) *Atg7* gene. Rescue of *Atg7* rescued the ability of aged mitochondria to maintain their membrane potential.

B. Proteomic analyses of carbonylated substrates. On the left proteins from *Atg7*$^{f/f}$ muscles; in the center proteins from *Atg7*$^{-/-}$ muscles; on the right: proteins from *Atg7*$^{-/-}$ muscles after treatment with anti-oxidant Trolox.

C. Muscle fibers from *Atg7*$^{-/-}$ muscles display less force than age-matched controls.

Figure S5. Trolox treatment did not rescue the atrophy of *Atg7*$^{-/-}$ mice, related to Figure 7.

Atrophy of *Atg7*$^{-/-}$ mice was not ameliorated upon anti-oxidant treatment.

Table S1

Protein spot no[a]	Protein	Swiss-Prot accession	Mascot score [c]	Sequence coverage (%)[d]	Matched Peptides[e]	Theoretical protein mass (Da)[g]	Theoretical PI[h]	RMI ratio[i] Atg$^{-/-}$/ Atg$^{f/f}$	RMI ratio Atg$^{-/-}$ Trolox / Atg$^{-/-}$
1	Aconitate hydratase	Q99KI0	283	30	7/18	85,464	8,1	1,56	0,28
2	Aconitate hydratase	Q99KI0	736	47	10/20	85,464	8,1	1,59	0,58
3	Aconitate hydratase	Q99KI0	192	17	5/10	85,464	8,1	1,42	>0,8
4	Aconitate hydratase	Q99KI0	168	9	5/7	85,464	8,1	1,56	>0,8
5	Glycogen phosphorylase, muscle form	Q9WUB3	172	23	5/17	97,286	6,7	3,76	0,55
6	Succinate dehydrogenase	Q8K2B3	395	47	10/20	72,585	7.06	1,65	0,35
7	Heat shock cognate 71 kDa protein	P63017	273	28	10/12	70,871	5,4	1,25	0,42
8	Pyruvate kinase isozymes M1/M2	P52480	688	50	8/20	57,845	7,2	2,44	0,66
9	Pyruvate kinase isozymes M1/M2	P52480	548	42	8/18	57,845	7,2	1,72	0,71
10	Desmin	P31001	487	48	11/18	53,498	5,2	3,78	0,23
10	Vimentin	P20152	57	4	2/2	53,688	5,1	3,78	0,23
11	Tubulin alpha-4A chain	P68368	117	27	6/8	49,924	5,0	3,16	0,47
12	Tubulin alpha-4A chain	P68368	61	6	2/2	49,924	5,0	1,30	0,44
13	Cytochrome b-c1 complex subunit 1	Q9CZ13	168	34	9/12	52,769	5,8	1,30	0,30
14	Cytochrome b-c1 complex subunit 1	Q9CZ13	87	24	2/10	52,769	5,8	2,72	0,57
15	ATP synthase subunit beta	P56480	902	59	12/20	56,300	5,2	2,44	0,51
16	ATP synthase subunit beta	P56480	732	50	12/18	56,300	5,2	1,39	0,46
17	Fructose-bisphosphate aldolase A	P05064	77	60	11/14	39,356	8,3	2,59	0,41
18	Actin, alpha skeletal muscle	P68134	810	47	7/12	42,051	5,2	1,35	0,67
19	Glyceraldehyde-3-phosphate dehydrogenase	P16858	812	42	7/8	35,810	8,4	1,3	0,32
20	Triosephosphate isomerase	P17751	1113	65	13/13	26,713	6,9	2,9	0,56
21	Triosephosphate isomerase	P17751	1148	65	13/13	26,713	6,9	1,4	0,48
22	Myoglobin	P04247	723	68	8/8	17,070	7,1	1,9	0,28

Table S1. Spots of interest identified by MS described in Experimental procedures and shown in Figure S4-B ,related to Figure 6 and Figure S4-B. Protein spots no (a) refer to numbered spots on Fig S6. For each spot, different parameters clarifying protein identification by MS are indicated [accession number (b), mascot score (c), % sequence coverage (d), no. of matched peptides (e), no. of sequenced peptides (f), theoretical protein mass (g) and theoretical PI (h)]. RMI ratio (i) represents the Relative Modification Index Ratio.

SUPPLEMENTAL EXPERIMENTAL PROCEDURES

Oligo sequence (5'-3').

shRNA oligos	Oligo sequence (5'-3')
p62/SQSTM1	Fw: TGCTGAGAGACTGGAGTTCACCTGTAGTTTTGGCCACTGACTGACTACAGGTGCTCCAGTCTCT Rev: CCTGAGAGACTGGAGCACCTGTAGTCAGTCAGTGGCCAAAACTACAGGTGAACTCCAGTCTCTC

Primers for quantitative Real Time PCR (qRT-PCR) analyses.

qRT-PCR primer	Oligo Sequence (5'-3')
m-AChRγ	Fw: CAGTGGGGGACCTAGAAACA Rev: ACCTTTCCAATCCACAGCAC
m-MuSK	Fw: ATCACCACGCCTCTTGAAAC Rev: TGTCTTCCACGCTCAGAATG
m-PAN-ACTIN	Fw: CTGGCTCCTAGCACCATGAAGAT Rev: GGTGGACAGTGAGGCCAGGAT
m-h-GAPDH	Fw: TGCACCACCAACTGCTTAGC Rev: GGCATGGACTGTGGTCATG

Antibodies

Primary Antibodies	**Company**
anti-ATG7	Sigma
anti-LC3	Sigma
anti-GAPDH	Abcam
anti-NCAM	Millipore
anti-P62	Sigma
anti-pan actin	Sigma
Secondary Antibodies	
anti-mouse Alexa Fluor 488 and 594	Life Technologies
anti-rabbit Alexa Fluor 488 and 594	Life Technologies
anti-mouse HRP Conjugate	Bio-rad
anti-rabbit HRP Conjugate	Bio-rad

Protein Carbonyls Detection and anti-oxidant treatment

For proteomic analyses, gastrocnemius muscle derived wild-type, Atg7 KO mice and Atg7 KO mice treated with Trolox (three animals per group), were homogenized in an UltratoraxTM homogenizer (low setting, 3 s) using a lysis buffer (10 mM tris-HCl (pH 7.4), 8 M urea, 2 M thiourea, 4% (w/v) CHAPS) and clarified by centrifugation. Proteins in the supernatant were precipitated using the 2-D Clean-Up kit (GE Healthcare) following the manufacturer instructions. Protein precipitates were then resuspended in lysis buffer and protein quantification was performed using the Bradford method (Pierce), using bovine serum albumin as a standard. Protein carbonyl detection was performed using OxyBlotTM, according to manufacturer instructions. For 1D Oxyblot, 15 µg of protein lysates were derivatized with 2,4dinitrophenylhydrazine followed by SDS-PAGE (12% (v/v) polyacrylamide) separation and electro blotting onto nitrocellulose membranes. After blocking, membranes were incubated with anti-DNP antibodies, washed, and incubated with peroxidase conjugated anti-rabbit IgG antibodies. 2D Oxyblot was performed in protein extracts derived from the same samples used for 1D Oxyblot, after 2D PAGE separation as described previously (Baraibar et al., 2011). For each sample two gels were performed in parallel, one for colloidal blue staining of total proteins and other for electroblotting onto nitrocellulose membranes. Membranes were then incubated for 2 h in the blocking solution and carbonyl detection was performed using the OxyBlotTM kit, as described above. Membranes were developed using Amersham ECL Plus Western Blotting Detection System. Films were digitized with UMAX UTA-100 scanner (GE Healthcare) and densitometry analyses were performed using NIH ImageJ or Image Master 2D Platinum 7 software (GE Healthcare).

2D-OxyBlot data acquisition and analysis.

For each spot identified by coomassie blue as well as from the OxyBlot a percentage volume was obtained in pixels (%Vol). The %Vol corresponds to a normalized value of the spot volume by considering the total volume of all the spots present in the gels or on films. %Vol of carbonylated spots from $Atg7^{f/f}$, $Atg7^{-/-}$, and $Atg7^{-/-}$ Trolox were normalized with %Vol of the corresponding Coomassie-stained spot to obtain a normalized %Vol (N%Vol). The N%Vol of spots derived from $Atg^{-/-}$ were divided by the N%Vol of $Atg7^{f/f}$ to obtain the Relative Modification Index ratio (RMI ratio). In addition the ratio $Atg7^{-/-}$ Trolox / $Atg7^{-/-}$ was performed after Trolox tratment. Spots with an RMI ratio ≥1.2 are considered as oxidatively modified in $Atg7^{-/-}$ and spots with a RMI ratio <0,8 are considered as decreased after Trolox treatment.

In-gel digestion, mass spectrometry protein identification and database searches.

Spots of interest were manually excised from gels and proteins were digested with trypsin. Peptide mass spectra were acquired in positive reflector mode on a 4800 Plus MALDI TOF/TOF™ Analyzer (Applied Biosystems, Foster City, CA, USA) using 20 kV of acceleration voltage. Each spectrum was externally calibrated using peptides derived by tryptic digestion of ß-lactoglobulin. Tandem mass spectra were acquired using the same instrument in MS/MS positive mode. Output peak lists were generated using Data Explorer (Applied Biosystems, Foster City, CA, USA) from the raw data. MS and MS/MS peak lists were combined into search files and used to search SwissProt database using the Mascot search engine (Matrix Science Ltd, London, UK). Search parameters were as follows: Database: SwissProt; Taxonomy: all entries or mammalian; Enzyme: trypsin; Allow up to 1 missed cleavage; Fixed modifications: none; Variable modifications: methionine oxidation; Peptide mass tolerance: 70 ppm; and Fragment mass tolerance: 500 ppm. Mascot protein scores greater than 56 are significant at $p<0.05$.